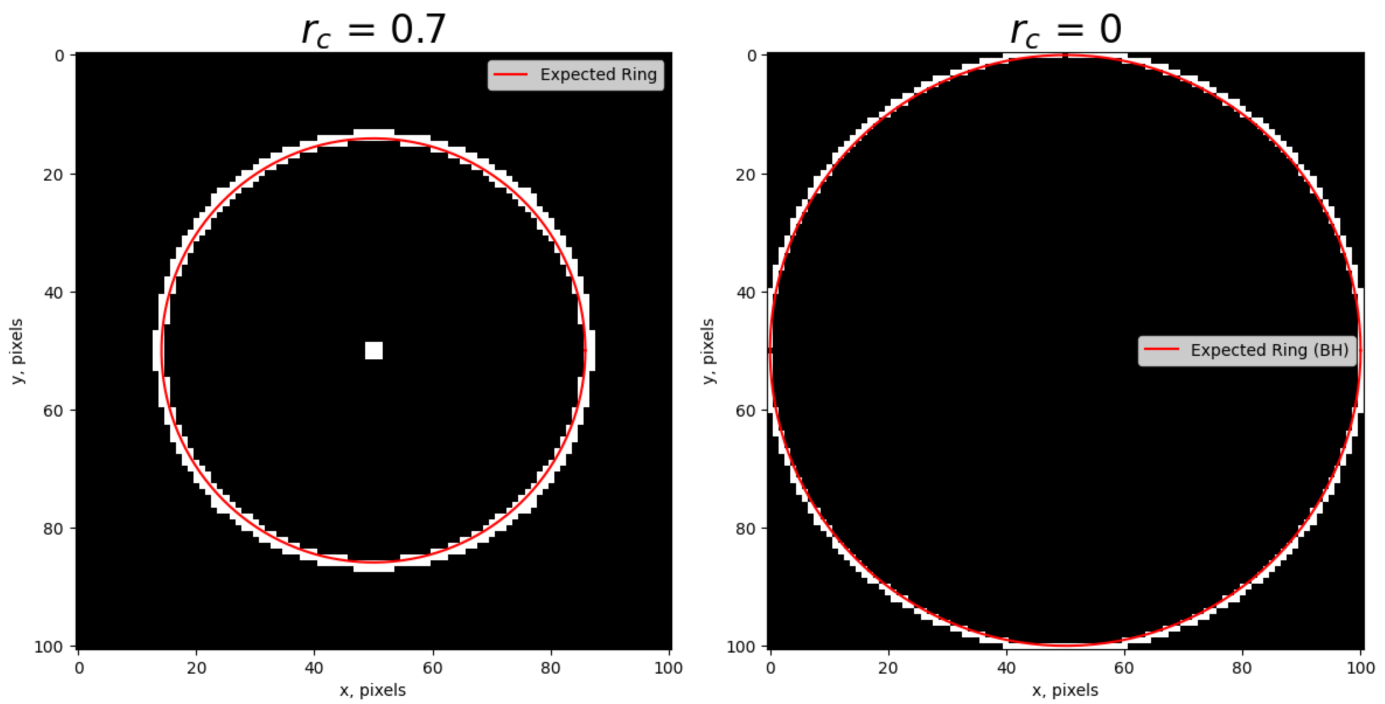

Figure 1: Validation Test, lensing of perfectly aligned point source

[LEFT]: source plane is an empty 2D image of size (101×101) containing a single central bright pixel, the source. Lens, which is modelled as an isothermal ellipsoid, is applied to the source plane with core radius $r_c = 0.7$ and ellipticity $\epsilon = 0$. Resulting pattern radius matches the expected radius for an Einstein ring, $r = \sqrt{1 - r_c^2}$.

[RIGHT]: r_c is reduced from 0.7 to 0, simulating a Schwarzschild Black Hole lens. The produced Einstein ring still matches the expected radius. Pattern pixels at the edges are clipped off from the pattern due to reduced coordinate transformations. Can increase reduced range from $(-1, 1)$ to see the whole pattern.

The figure produces a lensed pattern for a perfectly aligned point source, indicating successful completion of the validation test, allowing to introduce additional features.

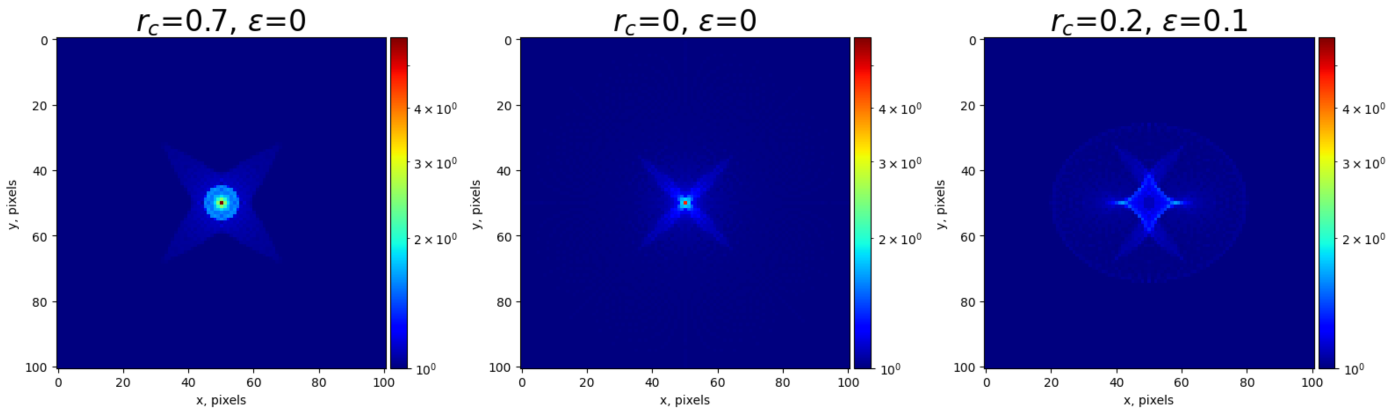

Figure 2: Shape distortion map

Shape distortions are parametrized as a ratio of the lensed pattern to the total area of the image for every possible alignment of the point source

[LEFT]: Distortion map for a circular lens with core radius $r_c = 0.7$. Distortion magnitude is radially symmetric with maximum value at the centre, e.g., perfectly aligned source. This indicates an Einstein ring to be the largest possible distortion in magnitude, as expected.

[MIDDLE]: r_c is reduced from 0.7 to 0. The distortion pattern magnitude is condensed to the central region. perfectly aligned source still produces an Einstein ring, however slightly misaligned sources do not result in as considerable distortions as for $r_c = 0.7$ lens.

[RIGHT]: Distortion map for a lens with $r_c = 0.2$; $\epsilon = 1$. Central source does not produce an Einstein ring anymore. Two separate spots of large magnitudes are equally spaced from the centre on the major axis while the central region produces almost no distortions.

The figure produces results that indicate which source alignment gives the most distorted image after lensing. Bright blue ‘star-like‘ regions surrounding the patterns are likely to mark lensing caustics.

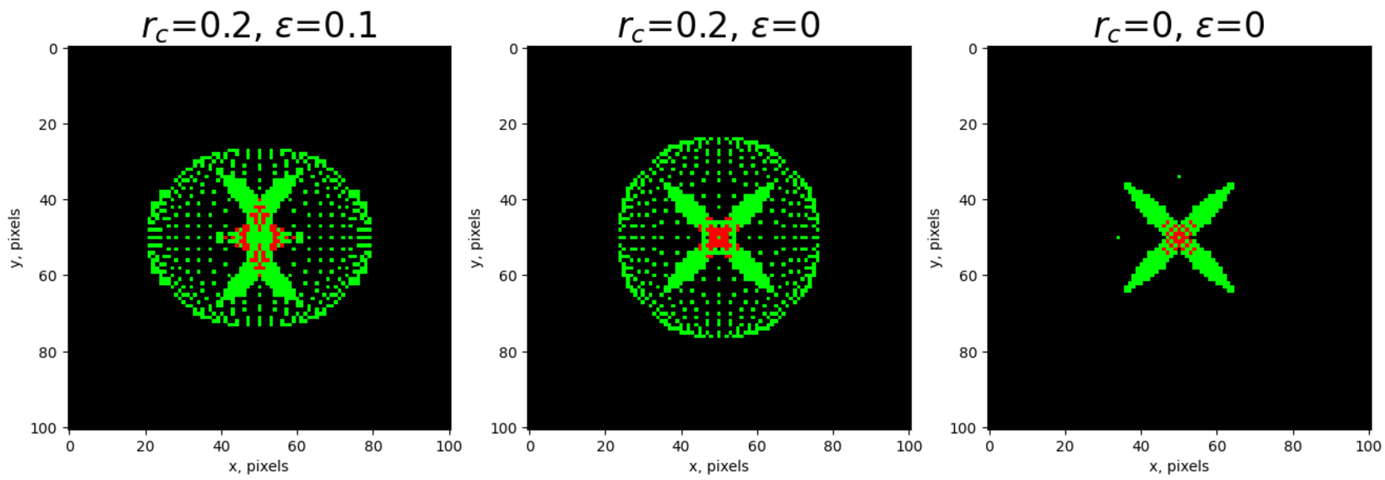

Figure 3: Lens Caustic study

Gravitational lensing Caustics are defined as regions that result in a point source producing two/three (outer caustic, GREEN) or more (inner caustic, RED) images when lensed (with Einstein ring as an exception).

[LEFT]: Caustic regions for a lens with $r_c = 0.2$; $\epsilon = 1$. Can see a similar pattern as for the corresponding lens in Figure 2. Bright blue regions there indeed mark lens caustics.

[MIDDLE]: Circular lens with $r_c = 0.2$ caustic patterns. The central point is marked green because an Einstein ring is a single shape. As before, caustics mark similar regions as the corresponding lens from Figure 2.

[RIGHT]: Distortion map Black Hole lens. A perfectly aligned source produces an Einstein ring only (see Figure 1, [RIGHT]) but is marked as a green spot, indicating that two shapes or more are formed. Also, two outlier points shifted from the centre along the Y and X axes are formed. These artefacts are likely to be due to numerical fluctuations.

The figure helps qualitatively explain the origin of puzzling centrally symmetric regions in Figure 2 by introducing concept of Gravitational Lens Caustics.

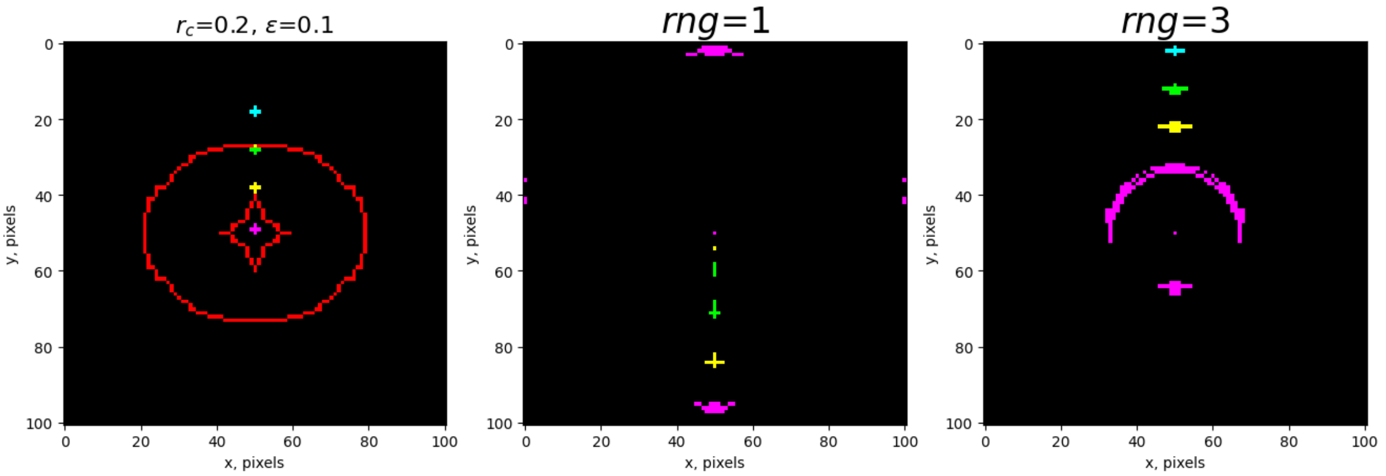

Figure 4: Visual effects of caustics

[LEFT]: Caustic regions contour for a lens with $r_c = 0.2$; $\epsilon = 1$. Empty image with four star-like sources of different colours. Positions are chosen specifically to be within or out of inner and outer caustics.

[MIDDLE]: Lensed image of the four sources. range of reduced coordinates is the default, $(-1, 1)$. The blue source is not visible due to the magnification of the lens. Only sources within the outer caustic are visible for range $(-1, 1)$.

[RIGHT]: Lensed image of the four sources, but the range is increased to $(-3, 3)$. This reduces the effective range of the lens, so that only the purple source remains within the caustic region. Remaining sources are still visible and distorted due to image not being magnified as much.

The figure indicates how resulting lens patterns can help determining the lens geometry by considering concept of caustics.

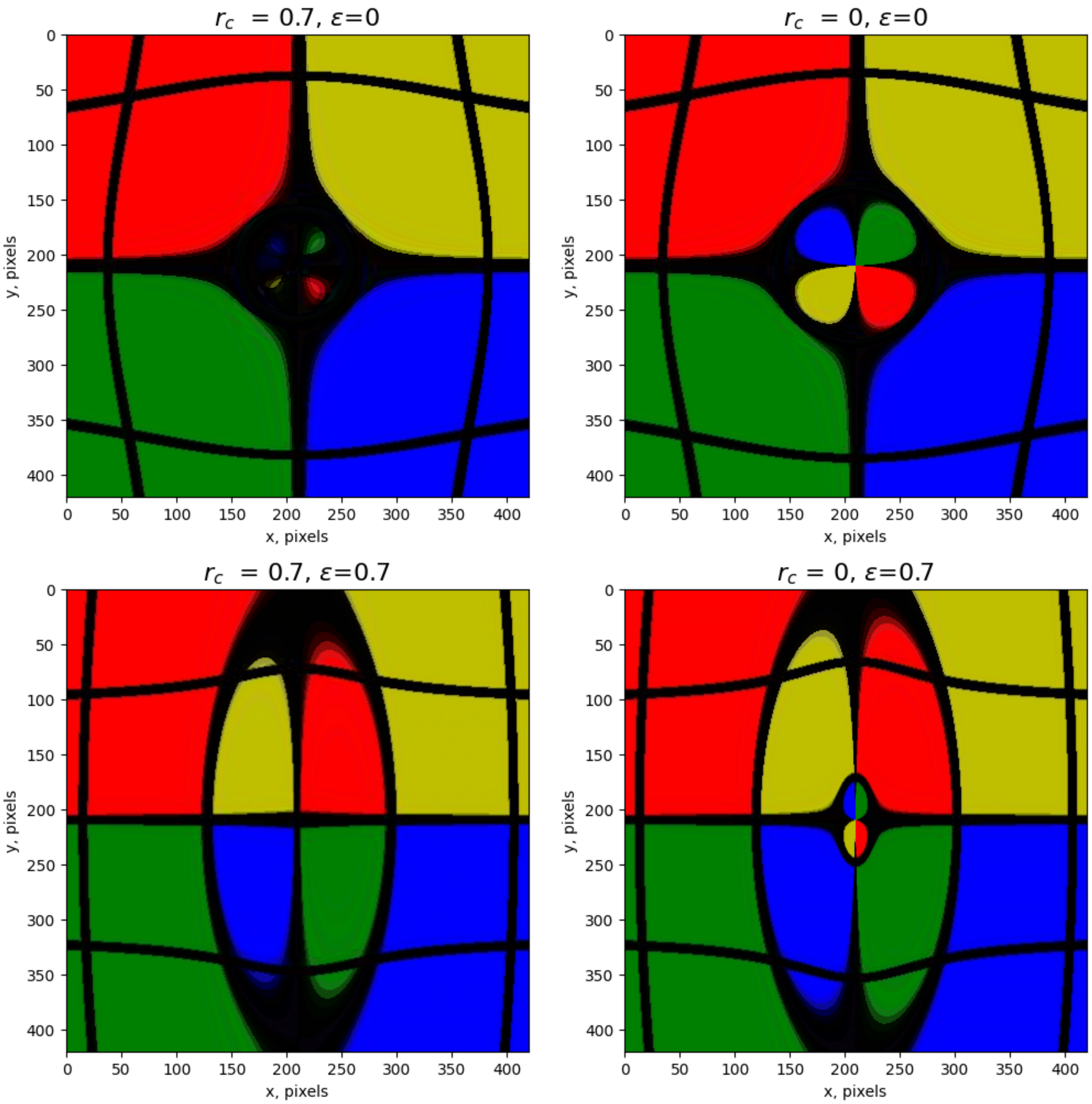

Figure 5: Geometry of distortions using a coloured chessboard.

Board of size (420×420) with 16 squares in total was used. In each corner, 4 corresponding squares were coloured into Red, Green, Yellow and Blue colours. Size was increased to improve quality.

[TOP-LEFT]: Lens with $r_c = 0.7$; $\epsilon = 0$. Geometry can be noted but the core reduces the visibility due to black line thickness

[TOP-RIGHT]: Reducing r_c to 0 solves the problem. Distortions are centrally symmetric for a circular lens with $r_c = 0$. Shape of red/green 'drops' is slightly bigger than that of blue/yellow ones because of imperfect centering of the image.

[BOTTOM-LEFT]: Lens with $r_c = 0.7$; $\epsilon = 0.7$. Symmetry is now axial, not central.

[BOTTOM-RIGHT]: Reducing r_c to 0 for elliptical lens results in more sophisticated patterns. Symmetry is now neither axial, nor central (mixture of both). For each colour, three separate images exist.

The figure qualitatively gives insight on what symmetry of distortions we can expect for different lens parameters.

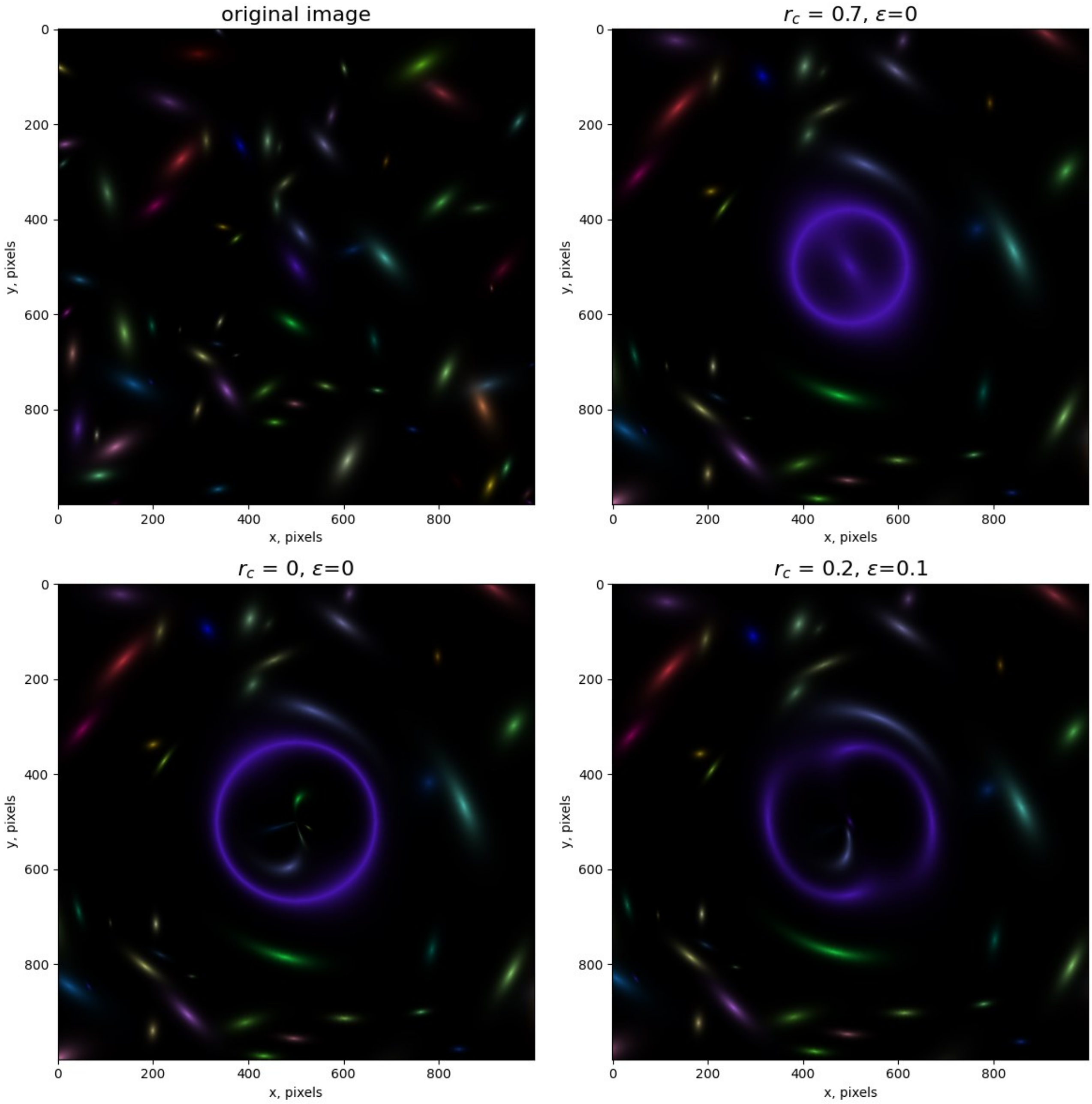

Figure 6: Random galaxy distribution lensing.

Source image of size (1001×1001) contains a random distribution of 70 galaxies with specified angles, RGB colours and exponentially decaying brightness profile. One galaxy is specifically placed at the centre to cause an Einstein ring.

[TOP-LEFT]: Original image, random galaxy distribution.

[TOP-RIGHT]: Lens with $r_c = 0.7$; $\epsilon = 0$. The range of reduced coordinates increased to $(-3, 3)$ to deal with magnification. Einstein Ring is produced as expected, observed distortions are similar to Figure 4 [RIGHT].

[BOTTOM-LEFT]: Lens with $r_c = 0$; $\epsilon = 0$. Reduced core radius allows to witness central symmetry as observed in Figure 5 [TOP-RIGHT], as well as same type of distortions (slight shear) for sources outside caustics.

[BOTTOM-RIGHT]: As expected, Einstein ring is disrupted for elliptical lens with $r_c = 02$; $\epsilon = 0.1$. Symmetry cannot be observed due to small value of ellipticity and insufficient number of sources close to the central region.

The figure brings previous concepts together as observed for a simulated image, bringing it closer to a real physical problem.

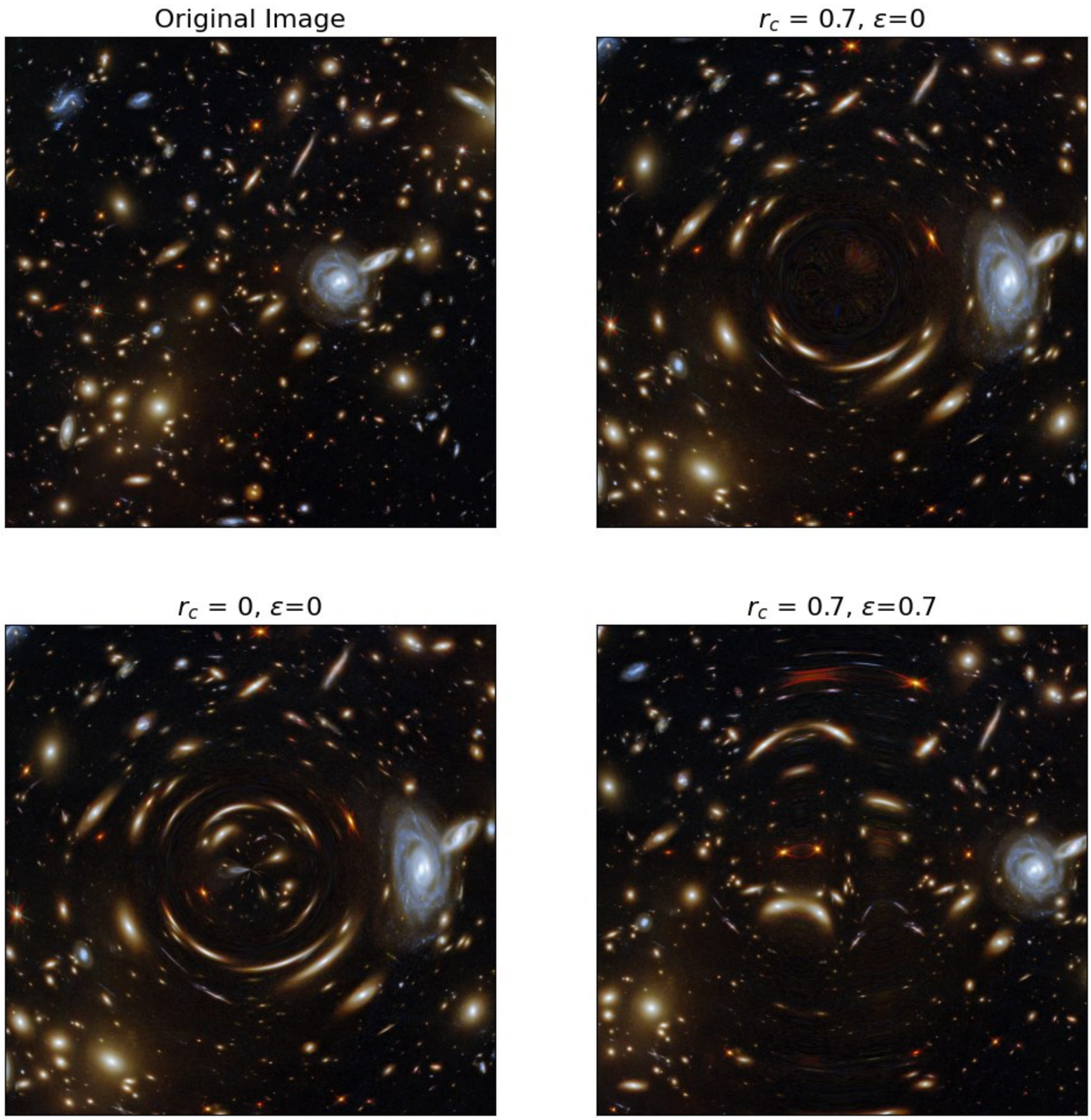

Figure 7: Lensing of a real galaxy cluster image.

Source image of size (2463×2463) is an image of galaxy cluster ACO S 295 captured by the Hubble Space Telescope. Source: [Hubble Gazes at a Galactic Menagerie]

[TOP-LEFT]: Original image, galaxy cluster ACO S 295.

[TOP-RIGHT]: Lens with $r_c = 0.7$; $\epsilon = 0$. The range of reduced coordinates increased to $(-3, 3)$ to deal with magnification. Big core radius does not allow to witness any previously observed symmetries in distortion.

[BOTTOM-LEFT]: Reduce r_c to 0. Reduced core radius allows to witness central symmetry as observed in Figure 5 [TOP-RIGHT], as well as same type of distortions (slight shear) for sources outside caustics.

[BOTTOM-RIGHT]: For elliptical lens with $r_c = 0.7$; $\epsilon = 0.7$, doubled images are created and resemble symmetry from Figure 5 [BOTTOM-RIGHT].

The figure compares the results acquired for real image to that of a simulated galaxy cluster.

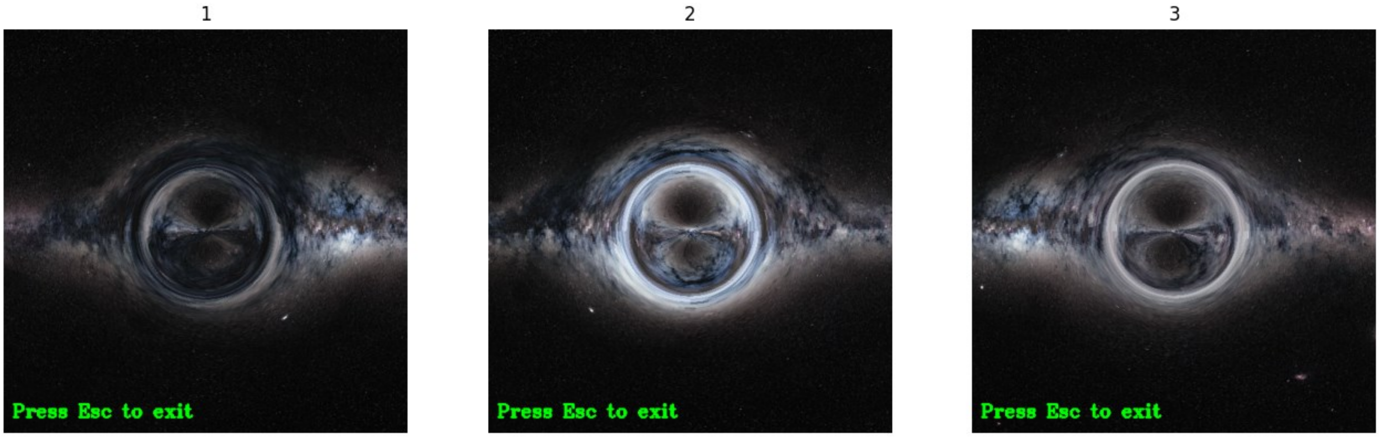

Figure 8: Milky Way moving through Schwarzschild Black Hole lens.

Image source: Milky Way 360 Panorama

Images are taken from a movie produced within the main code file. images are 300th, 400th and 500th frame of the movie respectively. Size of the image is (500×500).

Library used to produce a movie uses BGR colour scheme rather than RGB, hence blue colours are dominant in the figure.

The figure allows to witness application of previously described concepts and symmetries affecting the background image of the Milky Way galaxy. Einstein rings, axial and central images, as well as outside-caustic shear can be clearly visible in the movie.